ACS Photonics

Article

pubs.acs.org/journal/apchd5

Surface Lattice Resonances in Plasmonic Arrays of Asymmetric Disc Dimers

Alastair D. Humphrey, Nina Meinzer,* Timothy A. Starkey, and William L. Barnes

School of Physics and Astronomy, University of Exeter, Stocker Road, Exeter EX4 4QL, United Kingdom

Supporting Information

ABSTRACT: We study regular wavelength scale arrays of metallic dimers. By employing dimers made up of two different sized discs, we are able to couple to array-based collective surface lattice resonances of both bright and dark, that is symmetric and antisymmetric, dimer modes and to show that the degree of asymmetry can be used to control the relative strength of the two surface-lattice modes. The collective nature of these excitations can even lead to an antisymmetric surface-lattice resonance that is stronger than the symmetric one; this is in stark contrast to the dark and bright nature of the underlying modes of the individual dimers. We verify these experimental findings, derived from extinction measurements, by comparison with both analytical and numerical modeling.

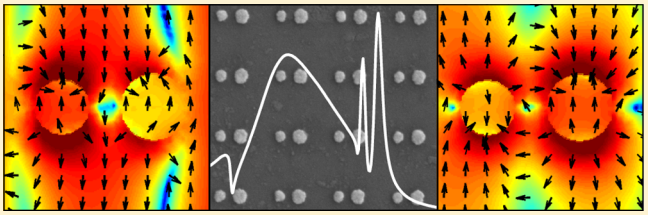

KEYWORDS: *plasmonics, surface-lattice resonances, dark modes, collective array resonances, nanoparticle array, near-field coupling*

The plasmon modes of individual metallic nanostructures depend sensitively on their shape, size, composition, and local environment.[1,2] When a number of metallic nanostructures are in close proximity, the plasmon modes interact with one another, leading to an overall response that can be significantly different from that of the isolated elements.[3] Near-field coupling between two closely spaced particles causes mode-hybridization,[4−6] whereas regular arrays of nanoantennas can support collective modes mediated by far-field interactions.[7−11] In both cases, the resulting resonances can be engineered to have much higher quality factors than those typically found for single plasmonic particles.

The mechanisms giving rise to the narrow resonances are fundamentally different for an isolated ensemble of near-field coupled particles and for extended, regular arrays of particles. In the first instance, the coupled resonators support a dark mode, that is, one with a vanishing dipole moment, which therefore does not couple to the far field. The particle ensemble thus becomes a high-quality resonator when excited in this state,[4,11,12] leading to strong field enhancements.[13,14] In the second case, the individual resonators form a periodic array with interelement distances on the order of the operating wavelength in which the electric fields from all scatterers can interact coherently and in phase with both each other and with the incident light. The collective modes of regular arrays, often known as surface lattice resonances[9,15−17] (SLRs), have shown potential for sensing[18] and lasing,[19] and have been successfully exploited in strong-coupling experiments;[20,21] they also show promise in mediating magnonic interactions between magnetic nanoparticles[22,23] and for solid-state lighting.[24] Very recently structured lattices have been used to demonstrate superlattice resonances,[25] opening an extra route to the control of optical properties; array structures have also been extended somewhat into the third dimension.[18,26] Here we investigate what happens when these two methods of producing narrow plasmonic resonances are combined.[27] We find that the collective effect of the lattice is able to overturn the bright/dark nature of the modes supported by an isolated ensemble of plasmonic particles. Our findings show that collective lattice effects offer a powerful way to control the properties of plasmonic particles and may find use in plasmonic metasurfaces, lasers, and biosensors among others.

In the work reported here we study regular arrays of asymmetric disc dimers (ADDs) and compare the results to previous work on arrays of symmetric disc dimers.[28,29] The plasmon modes of a metallic dimer hybridize to give two nondegenerate modes: a bright mode where the oscillating dipole moments associated with the two particles (discs) are in phase and a dark mode where they are out of phase. For normal-incidence illumination, the dark mode of such symmetric dimers is not radiatively coupled, and the response is dominated by the bright mode. Breaking the symmetry of the base element by fabricating dimers made up of two discs with different diameters allows us to controllably introduce radiative coupling to the dark mode[30,31] (making it gray). The dark mode of the ADD may then lead to the formation of a second SLR in addition to the one associated with the bright (symmetric) mode. A typical example of the arrays of plasmonic asymmetric disc dimers we studied is shown in Figure 1a.

Let us first describe the optical response of the base element, that is, of an individual asymmetric disc dimer, in more detail: A closely spaced pair of plasmonic oscillators is coupled via the

Received: December 18, 2015
Published: March 4, 2016

DOI: 10.1021/acsphotonics.5b00727
ACS Photonics 2016, 3, 634−639

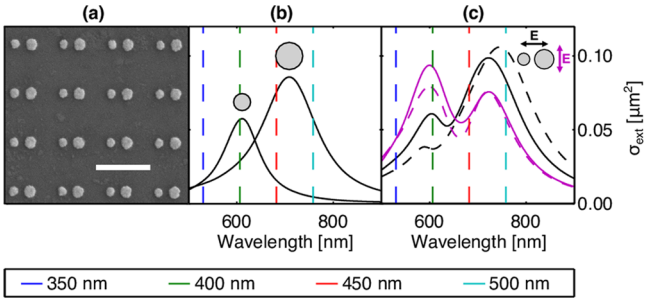

Figure 1. Asymmetric disc dimer (ADD). (a) Electron micrograph of a typical ADD array with a lattice constant a = 450 nm. The base elements are made up of two discs with diameters d_1 = 85 nm, d_2 = 115 nm, height h = 30 nm, and a center-to-center separation c = 150 nm. The scale bar is 500 nm. (b) Calculation of extinction spectra of the two single discs and (c) of the individual ADD, using a coupled dipole approach, for incident polarization parallel and perpendicular to the pair axis for two different disc spacings c = 150 nm (solid lines) and c = 110 nm (dashed lines). In both panels, the spectral position of the diffraction edge for the lattice constants considered are indicated by dashed colored lines.

overlapping near-fields and supports two distinct modes described by mode-hybridization.[4] In a simple picture, one can reduce the individual plasmon resonances to their associated dipole moments and consider how these couple. The two modes are thus identified as a symmetric solution, where the dipoles oscillate in phase, and an antisymmetric solution, where the dipoles have a π phase difference. While the symmetric mode radiates strongly because of its enhanced net dipole moment, the out-of-phase dipoles of the antisymmetric mode cancel, resulting in a zero net dipole moment, and the mode is therefore dark and does not radiate.

However, such modes are only truly dark under perfect symmetry conditions, and if these conditions are broken, for example, by oblique incidence of the exciting wave, leading to retardation across the structure, or by introducing a substrate with an index-mismatch to the superstrate, the mode becomes somewhat radiative with a small but nonvanishing net dipole moment, leading to potentially high-quality but usually weak (gray) resonances. In the asymmetric disc dimer that we use as the base element for our experiments, the necessary symmetry breaking takes the form of a geometric asymmetry, where one particle is smaller than the other.

This naturally raises the question of whether we observe the modes of a coupled dimer or simply the superposition of the two resonances of the two individual discs, which occur at slightly different spectral positions. A comparison of Figure 1b and c shows the, albeit small, mode-splitting of the coupled system relative to the individual resonances: While the two resonances of the single discs occur at 612 and 709 nm (separation $\Delta\lambda$ = 97 nm), the two hybridized modes of the disc dimer are found at 596 and 725 nm, giving a wavelength separation $\Delta\lambda$ = 129 nm, which shows an additional mode splitting, indicative of coupling. This splitting increases to $\Delta\lambda$ = 155 nm for smaller separation of the discs (c = 110 nm, dashed lines in Figure 1c), corresponding to stronger coupling. However, the signature of a coupled system is more clearly seen in the difference between the two spectra shown for the dimer (Figure 1c) when excited with incident light polarized with the electric field parallel (black line) and perpendicular (magenta line) to the pair axis. In these extinction-cross-section spectra, the strength of the two resonances are reversed for the different polarizations: The short-wavelength resonance is stronger for perpendicular (magenta) than for parallel (black) polarization and vice versa for the long-wavelength peak. If these were the resonances of the individual discs, the weaker resonance would always be that of the smaller particle (shorter wavelength) because of its smaller polarizability, whereas in a coupled pair, the weaker resonance is associated with the antisymmetric, that is, gray resonance. Whether the weaker resonance is the short- or long-wavelength solution depends on the exact coupling conditions: In a longitudinally coupled dipole pair (parallel polarization), the antisymmetric mode occurs at a shorter wavelength than the symmetric mode, in the transversally coupled case (perpendicular polarization) it is the other way around. We can thus conclude that the two modes observed stem from the near-field coupled ADD base elements.

SURFACE LATTICE RESONANCES IN ADD ARRAYS

The main focus of this report is on the interaction of such ADD elements within periodic arrangements. We fabricated square arrays of ADDs (d_1 = 85 nm, d_2 = 115 nm, h = 30 nm, c = 150 nm) with different lattice constants a, ranging from 350 to 500 nm and measured their extinction spectra in an index-matched (n = 1.515) environment. The values of a were chosen so that the diffraction edge, that is, the wavelength separating the nondiffractive from the diffractive regime, occurs below, between, and above the two resonances of the ADDs, as indicated by the dashed colored lines in Figure 1a,b.

The results of these measurements are presented in Figure 2 for incident polarization parallel (a) and perpendicular (b) to the dimer axis, together with the corresponding calculations (c, d) based on an analytical dipole model[32−35] (S-factor model), for which we have modified the calculation of the S-factor for an array with a two-element basis discussed in ref 29 to take

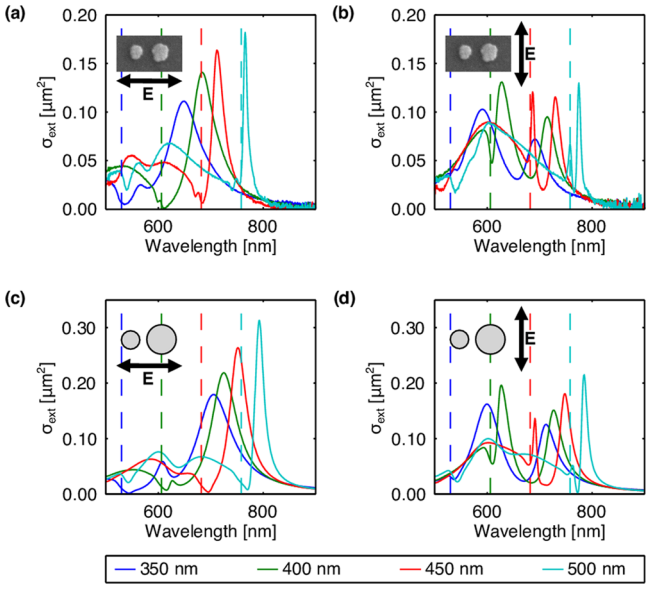

Figure 2. Extinction cross-section spectra of ADD arrays with different lattice constants a. (a, b) Experimental results for incident polarization (a) parallel and (b) perpendicular to the dimer axis. (c, d) Spectra derived from S-factor model calculations for incident polarization (c) parallel and (d) perpendicular to the dimer axis. The positions of the diffraction edge for all spectra are indicated by vertical dashed lines in the same color as the corresponding data set. All extinction cross-sections are normalized to the unit cell containing one base element.

DOI: 10.1021/acsphotonics.5b00727
ACS Photonics 2016, 3, 634−639

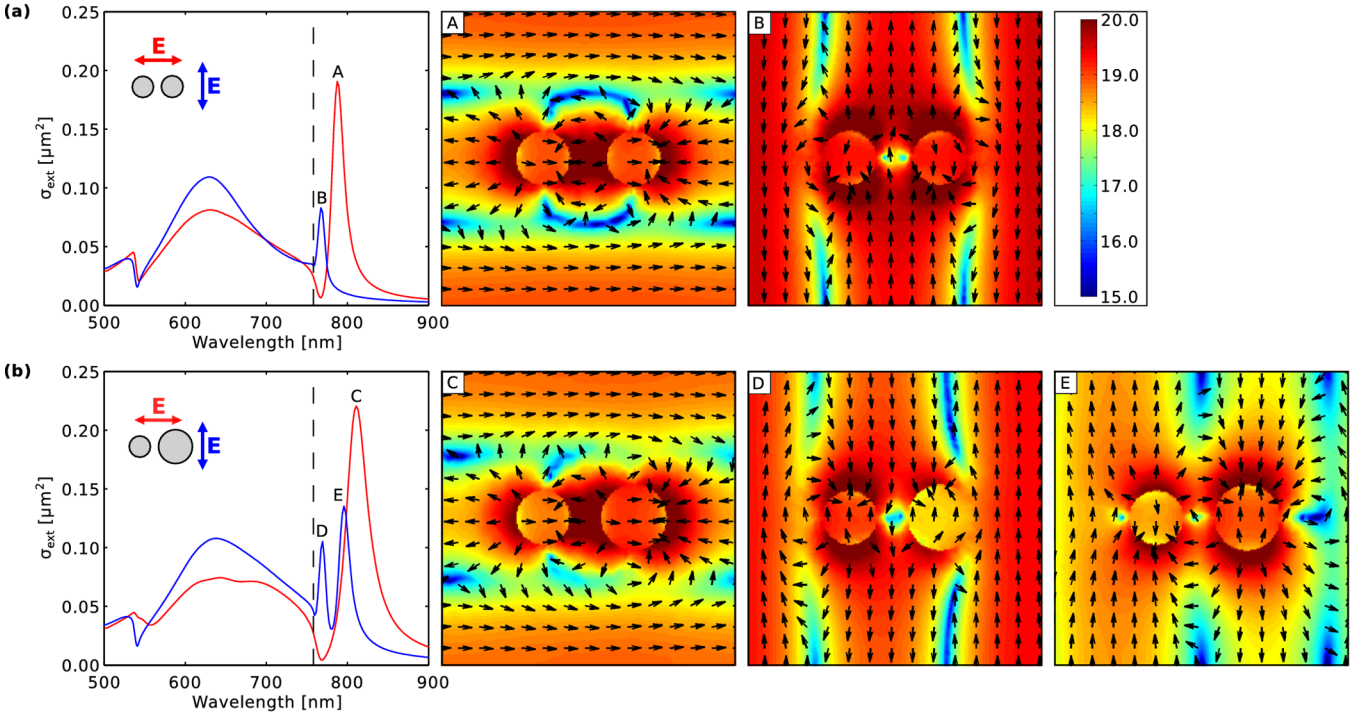

Figure 3. Finite-element models. Extinction spectra and electric field distributions (as $\log(E/E_0)$) in the symmetry plane of the structures for the different resonance positions are shown for an array (a = 450 nm) of (a) symmetric disc dimers ($d_1 = d_2$ = 90 nm, c = 150 nm) and of (b) asymmetric disc dimers (d_1 = 90 nm, d_2 = 110 nm, c = 150 nm). In the extinction spectra, red lines correspond to incident polarization parallel and blue lines to polarization perpendicular to the dimer axis. The field maps for modes A−E depict the total electric field, that is, the sum of incident and resonantly scattered field.

into account different dipole moments for the two particles in the basis (see methods and Supporting Information for details). The two S-factors S and S', which are related to the two sublattices, can be calculated from the distinct, yet coupled, effective polarizabilities α_1^* and α_2^* of the two particles in the basis, which are given by

$$\alpha_{1,2}^* = \frac{\alpha_{1,2}(1 - \alpha_{2,1}\varepsilon_0 S + \alpha_{2,1}\varepsilon_0 S')}{(1 - \alpha_1\varepsilon_0 S)(1 - \alpha_2\varepsilon_0 S) - \alpha_1\alpha_2(\varepsilon_0 S')^2} \quad (1)$$

where α_1 and α_2 are the polarizabilities of the two isolated particles that make up the ADD.

For both orientations of the incident electric field the shape and strength of the SLR depends on the position of the diffraction edge relative to the single-element resonances. When the lattice constant is not large enough to allow diffractive coupling (a = 350 nm, blue line), the spectrum of the array resembles that of the individual base element (compare Figure 1c). The data show two relatively broad resonances whose relative strengths are reversed for parallel (a, c) and perpendicular (b, d) incident polarization, as expected from the single-element response (Figure 1c). Increasing the lattice constant a shifts the position of the diffraction edge toward longer wavelengths and SLRs occur due to diffractive coupling. The resonances become increasingly sharp and pronounced, reaching a maximum quality factor when the diffraction edge is located on the long-wavelength tail of the single-element resonance,[9] corresponding to the cyan spectra in Figure 2.

These observations about how the shape and strength of the surface lattice resonance depend on the relative spectral position of the diffraction edge and the isolated plasmon resonance apply to both polarizations and to SLRs in general.[32,36] There is, however, one striking difference between the two polarizations in the case of ADD arrays: The spectra exhibit only a single SLR for parallel polarization (Figure 2a,c), whereas for an incident electric field perpendicular to the dimer axis, the spectra show double SLRs, reflecting the two modes of the ADD base element (Figure 2b,d). In contrast to the single-element or the nondiffractive case, the antisymmetric (longer wavelength) mode is the stronger mode in the double SLR for the given ADD.

This is, at first, surprising, as one expects the mode associated with a smaller net dipole moment (for the individual ADD) to couple to the far field less efficiently. However, as a collective array resonance, the strength of the SLR features depends not only on the mode supported by the base element, but also on the interaction of the scattered fields from all elements in the array, more precisely, on the net electric field at the site of one dimer by scattering arising from the other dimers. For the square array considered here, the contributions from elements along the array axes will be out of phase with the contributions from off-axis elements, leading to destructive interference. Further calculations show that these out-of-phase scattered fields from off-axis elements are stronger for wavelengths around or below the diffraction edge (see Supporting Information). Consequently, any mode corresponding to these wavelengths will be damped. For the case of parallel polarization, this effect leads to the antisymmetric (short-wavelength) mode being completely suppressed by comparison with the dominant symmetric mode, resulting in a single SLR.

The experimental data presented in Figure 2a,b qualitatively agree with the spectra calculated on the basis of a modified S-factor model (see Methods and Supporting Information for details) shown in Figure 2c,d, while the absolute values of the extinction cross-section per particle are approximately 1.5 times

DOI: 10.1021/acsphotonics.5b00727
ACS Photonics 2016, 3, 634−639

higher in the calculations than in the experiment. This is a systematic error in the modeling that uses the modified long-wavelength approximation[37] to analytically calculate the polarizability of the silver discs, which reaches the limits of its applicability for the particle sizes and wavelengths considered in this work.[29] However, the agreement between experimental and modeling data presented in this article is far better than in previous work,[29] where an additional error was added by using a wrong equation to calculate the extinction cross-section.

FIELD CHARACTERISTICS OF SLR MODES

To better establish the interpretation of our experimental data and to verify the conclusions we have drawn from the simple coupled-dipole picture (*S*-factor model), we also calculated extinction spectra and the electric field distributions associated with the observed modes using finite-element modeling for both a symmetric and an asymmetric dimer as the base element, as shown in Figure 3. These calculations confirm our main observation that a regular array of asymmetric disc dimers can support two SLRs.

Arrays with a symmetric dimer basis show a single SLR regardless of the incident polarization and the electric field plots for modes A and B in Figure 3a identify them as the coherent, constructive interference of the symmetric mode. For a perfectly symmetric base element, the dipole moments of the two resonators exactly cancel, resulting in a dark mode. It is nonradiative and can therefore not lead to an SLR produced by diffractive far-field coupling between the elements. Conversely, arrays comprised of asymmetric disc dimers also have one SLR for a field parallel to the dimer axis (red line in Figure 3b), but exhibit two SLRs for an incident electric field perpendicular to the dimer axis (blue line in Figure 3b). The corresponding electric field distributions reinforce our previous reasoning that the single SLR for parallel polarization is associated with the symmetric mode of the dimer (mode C), whereas the double SLR observed with perpendicular polarization reproduces both the symmetric (mode D) and the antisymmetric mode (mode E) of the ADD.

INFLUENCE OF ASYMMETRY

So far we have only considered one particular ADD as a base element (d_1 = 85 nm, d_2 = 115 nm, c = 150 nm) and compared it to arrays of symmetric dimers. We next want to examine what influence the degree of asymmetry within the ADD could have on the overall optical response of the array. We therefore fabricated several samples with identical lattice constant a = 500 nm but with different aspect ratios of the two discs in the ADD element; the interparticle distance, c = 150 nm, and the diameter of one particle, d_1 = 90 nm, remain the same, but the diameter of the second particle is varied between d_2 = 70 nm and d_2 = 125 nm.

Before we discuss the influence of the asymmetry on the SLRs, it is necessary to first review how the optical response of an individual ADD changes with the degree of asymmetry. If the size of one disc is kept constant, a change in the size of the second disc has two consequences: The spectral position of the two modes red-shifts with growing disc size and the net dipole moment for both the symmetric and the antisymmetric combination changes. In the symmetric case the net dipole moment increases, in line with the increase of the dipole moment of the individual disc. In the antisymmetric case, it is the difference between the two individual moments that is important. The net dipole moment takes a minimum value of zero when the discs are the same size. When the discs are of different sizes, the net moment not only depends on the difference in size (the aspect ratio), it also depends on the absolute value of the dipole moments of the two particles; for a given aspect ratio, the net dipole moment is greater when the two particles are larger. These general trends are the same for longitudinal and transverse coupling between the dipoles.

These considerations allow us to explain the changes observed in the associated SLRs, measurements of which are given in Figure 4 for four different values of d_2. The single SLR

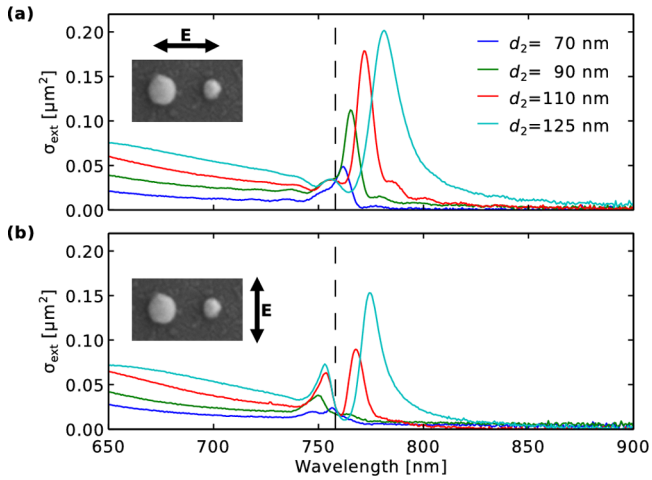

Figure 4. Measured extinction (per base element) spectra for varying degrees of asymmetry in the base element. The arrays are excited with polarization (a) parallel and (b) perpendicular to the particle-pair axis. In all samples, the lattice constant is a = 500 nm and the diameter of one particle and the interparticle distance in the dimer are constant at d_1 = 90 nm and c = 150 nm, while the diameter of the second particle is varied. The dashed black line indicates the position of the diffraction edge.

(Figure 4a) observed under polarization parallel to the pair axis slightly red-shifts and increases in strength with the growing size of the second particle, directly reflecting the behavior of the base element. Similarly, we find a general red-shift of the double SLR (Figure 4b) for perpendicular polarization as the second disc becomes larger. The relative strength of the symmetric and antisymmetric SLR also changes with a varying degree of asymmetry and overall disc size. While the short-wavelength, symmetric, SLR is stronger for smaller discs in the ADD, the antisymmetric SLR becomes more and more prominent with increasing values of d_2, thus, increasing net dipole moment, until it becomes the stronger of the two modes for d_2 = 110 nm. Note that for the special case of a symmetric pair (d_2 = d_1, green line in Figure 4b) the long-wavelength SLR disappears completely because the antisymmetric mode cannot couple to the far field.

CONCLUSION

We have studied the rich behavior of surface-lattice resonances in regular arrays formed from asymmetric disc dimers. Depending on the polarization of the incident light with respect to the dimer axis, such arrays show either a single or a double SLR associated with the symmetric and antisymmetric mode of the base element. The spectral position and the overall strength, as well as the relative strength of the two modes

DOI: 10.1021/acsphotonics.5b00727
ACS Photonics 2016, 3, 634−639

within this double SLR, can be adjusted by changing the geometry of the base element to such an extent that it is possible to excite strong collective modes with an antisymmetric character. These findings extend the potential of plasmonic arrays by offering an additional approach to controlling optical properties. In addition to the potential for sensing, lasing, solid-state lighting and magnonic effects discussed above, interesting opportunities involving chiral structures also exist.[25] These, together with the potential for various types of array fabrication, including DNA assembly[38] and substrate conformal imprint lithography,[24] indicate the significant potential for plasmonic arrays involving lattice resonances.

METHODS

Fabrication. Arrays of silver asymmetric disc dimers were fabricated by electron-beam lithography on fused silica substrates with subsequent thermal evaporation of a 30 nm silver layer, followed by a standard lift-off procedure.

Measurements. Extinction measurements were performed using an imaging spectrometer (Acton SpectraPro-2500i) attached to an inverted microscope (Nikon ECLIPSE TE2000-U), which had been modified to reduce the illumination spot to a diameter of 30 μm with a beam divergence of approximately 1°. All samples were index-matched to the substrate (n = 1.515) to provide a homogeneous environment. To facilitate comparison with the calculations, the extinction spectrum was converted into an extinction cross-sections per particle by normalizing to the area of a unit cell.

***S*-Factor Modeling.** We calculated the extinction spectra for arrays of particles (Figure 2c,d) using a simplified form of the coupled-dipole approximation, known as *S*-factor modeling: First, the polarizability of each particle is determined from the modified long-wavelength approximation.[37] Then, to find the response of the complete array, a particle in the center of the array is selected, and the sum of the scattered field from all surrounding particles (the *S*-factor) at this center position is calculated, treating all particles as point-like dipole scatterers. Finally, we convolve the spectra with a Gaussian of seven points, where each point corresponds to 1 nm, to mimic the binning procedure over pixel size in the experiment.

For arrays comprising a more complex basis than a single particle, it is not immediately clear whether the modeling ought to treat the two-particle basis as a single unit with a net dipole moment and then consider the effects of the array, or to treat them as two coupled subarrays with a single-particle basis each. The latter turns out to be correct, as discussed in more detail in ref 29. We have further modified the approach described therein to enable calculations of subarrays with different base particles like the ADD presented in this work, which leads to eq 1 and is further elaborated on in the Supporting Information.

Full-Wave Numerical Modeling. The spectra and field maps presented in Figure 3 were calculated using the commercial finite-element software ANSYS HFSS. The disc dimers are modeled as silver (permittivity values taken from ref 39) cylinders embedded in a homogeneous environment with a refractive index n = 1.515 and assumed to form an infinite array by applying periodic Floquet boundary conditions. We excite the sample with a plane wave under normal incidence, calculate the extinction as $1 - T$, and obtain the extinction cross-section by normalization to the size of the unit cell.

ASSOCIATED CONTENT

Supporting Information

The Supporting Information is available free of charge on the ACS Publications website at DOI: 10.1021/acsphotonics.5b00727. All data underlying the research presented in this paper can be accessed free of charge from the Open Research Exeter (ORE) database at DOI: hdl.handle.net/10871/20358.

Derivation of the polarizability (eq 1) used to calculate the collective response of the ADD arrays, as well as a discussion of the influence of off-axis elements on the strength of the lattice resonances observed (PDF).

AUTHOR INFORMATION

Corresponding Author

*E-mail: n.meinzer@exeter.ac.uk.

Notes

The authors declare no competing financial interest.

ACKNOWLEDGMENTS

The authors would like to acknowledge funding from The Leverhulme Trust and from the Engineering and Physical Sciences Research Council (U.K.) through the Programme Grant EP\I034548/1 (QUEST) and through Grant EP/K041150/1.

REFERENCES

(1) Mock, J. J.; Barbic, M.; Smith, D. R.; Schultz, D. A.; Schultz, S. Shape effects in plasmon resonances of individual colloidal silver nanoparticles. *J. Chem. Phys.* **2002**, *116*, 6755.

(2) Kelly, K. L.; Coronado, E.; Zhao, L. L.; Schatz, G. C. The Optical Properties of Metal Nanoparticles: The Influence of Size, Shape and Dielectric Environment. *J. Phys. Chem. B* **2003**, *107*, 668−677.

(3) Verre, R.; Yang, Z. J.; Käll, M. Optical Magnetism and Plasmonic Fano Resonances in Metal-Insulator-Metal Oligomers. *Nano Lett.* **2015**, *15*, 1952−1958.

(4) Prodan, E.; Radloff, C.; Halas, N. J.; Nordlander, P. A Hybridization Model for the Plasmon Response of Complex Nanostructures. *Science* **2003**, *302* (5644), 419−422.

(5) Rechberger, W.; Hohenau, A.; Leitner, A.; Krenn, J. R.; Lamprecht, B.; Aussenegg, F. R. Optical properties of two interacting gold nanoparticles. *Opt. Commun.* **2003**, *220*, 137−141.

(6) Dahmen, C.; Schmidt, B.; von Plessen, G. Radiation Damping in Metal Nanoparticle Pairs. *Nano Lett.* **2007**, *7*, 318−322.

(7) Pinchuk, A. O.; Schatz, G. C. Nanoparticle optical properties: Far- and near-field electrodynamic coupling in a chain of silver spherical nanoparticles. *Mater. Sci. Eng., B* **2008**, *149*, 251−258.

(8) Fedotov, V. A.; Rose, M.; Prosvirnin, S. L.; Papasimakis, N.; Zheludev, N. I. Sharp Trapped-Mode-Resonances in Planar Metamaterials with a Broken Structural Symmetry. *Phys. Rev. Lett.* **2007**, *99*, 147401.

(9) Auguié, B.; Barnes, W. L. Diffractive coupling in gold nanoparticle arrays and the effect of disorder. *Opt. Lett.* **2009**, *34*, 401−403.

(10) Meinzer, N.; Barnes, W. L.; Hooper, I. R. Plasmonic meta-atoms and metasurfaces. *Nat. Photonics* **2014**, *8*, 889−898.

(11) Collin, S. Nanostructure arrays in free-space: optical properties and applications. *Rep. Prog. Phys.* **2014**, *77*, 126402.

(12) Zhang, S.; Genov, D. A.; Wang, Y.; Liu, M.; Zhang, X. Plasmon-Induced Transparency in Metamaterials. *Phys. Rev. Lett.* **2008**, *101*, 047401.

(13) Hao, F.; Nordlander, P.; Sonnefraud, Y.; Van Dorpe, P.; Maier, S. A. Tunability of Subradiant Dipolar and Fano-Type Plasmon Resonances in Metallic/Disk Cavities: Implications for Nanoscale Optical Sensing. *ACS Nano* **2009**, *3*, 643−652.

DOI: 10.1021/acsphotonics.5b00727
ACS Photonics 2016, 3, 634−639

(14) Kravets, V. G.; Zoriniants, G.; Burrows, C. P.; Geim, A. K.; Barnes, W. L.; Grigorenko, A. N. Composite Au Nanostructures for Fluorescence Studies in Visible Light. *Nano Lett.* **2010**, *10*, 874−879.
(15) Luk'yanchuk, B.; Zheludev, N. I.; Maier, S. A.; Halas, N. J.; Nordlander, P.; Giessen, H.; Chong, C. T. The fano resonance in plasmonic nanostructures and metamaterials. *Nat. Mater.* **2010**, *9*, 707−715.
(16) Auguié, B.; Barnes, W. L. Collective resonances in gold nanoparticle arrays. *Phys. Rev. Lett.* **2008**, *101*, 143902.
(17) Kravets, V. G.; Schedin, F.; Grigorenko, A. N. Extremely Narrow Plasmon Resonances Based on Diffraction Coupling of Localized Plasmons in Arrays of Metallic Nanoparticles. *Phys. Rev. Lett.* **2008**, *101*, 087403.
(18) Thackray, B. D.; Kravets, V. G.; Schedin, F.; Auton, G.; Thomas, P. A.; Grigorenko, A. N. Narrow Collective Plasmon Resonances in Nanostructure Arrays Observed at Normal Light Incidence for Simplified Sensing in Asymmetric Air and Water Environments. *ACS Photonics* **2014**, *1*, 1116−1126.
(19) Zhou, W.; Dridi, M.; Suh, J. Y.; Kim, C. H.; Co, D. T.; Wasielewski, M. R.; Schatz, G. C.; Odom, T. W. Lasing action in strongly coupled plasmonic nanocavity arrays. *Nat. Nanotechnol.* **2013**, *8*, 506−511.
(20) Väkeväinen, A. I.; Moerland, R. J.; Rekola, H. T.; Eskelinen, A.-P.; Martikainen, J.-P.; Törmä, P. Plasmonic surface lattice resonances at the strong coupling regime. *Nano Lett.* **2014**, *14*, 1721−1727.
(21) Vecchi, G.; Giannini, V.; Gómez Rivas, J. Shaping the Fluorescent Emission by Lattice Resonances in Plasmonic Crystals of Nanoantennas. *Phys. Rev. Lett.* **2009**, *102*, 146807.
(22) Maccaferri, N.; Inchausti, X.; García-Martín, A.; Cuevas, J. C.; Tripathy, D.; Adeyeye, A. O.; Vavassori, P. Resonant Enhancement of Magneto-Optical Activity Induced by Surface Plasmon Polariton Modes Coupling in 2D Magnetoplasmonic Crystals. *ACS Photonics* **2015**, *2*, 1769−1779.
(23) Kataja, M.; Hakala, T. K.; Julku, A.; Huttunen, M. J.; van Dijken, S.; Törmä, P. Surface lattice resonances and magneto-optical response in magnetic nanoparticle arrays. *Nat. Commun.* **2015**, *6*, 7072.
(24) Lozano, G.; Louwers, D. J.; Rodríguez, S. R. K.; Murai, S.; Jansen, O. T. A.; Verschuuren, M. A.; Gómez Rivas, J. Plasmonic for solid-state lighting: Enhanced excitation and directional emission of highly efficient light sources. *Light: Sci. Appl.* **2013**, *2*, e66.
(25) Wang, L.-Y.; Smith, K. W.; Dominguez-Medina, S.; Moody, N.; Olson, J. M.; Zhang, H.; Chang, W.-S.; Kotov, N.; Link, S. Circular Differential Scattering of Single Chiral Self-Assembled Gold Nanorod Dimers. *ACS Photonics* **2015**, *2*, 1602−1610.
(26) Zilio, P.; Malerba, M.; Toma, A.; Zaccaria, R. P.; Jacassi, A.; De Angleis, F. Hybridization in Three Dimensions: A Novel Route toward Plasmonic Metamolecules. *Nano Lett.* **2015**, *15*, 5200−5207.
(27) Giannini, V.; Vecchi, G.; Gómez Rivas, J. Lighting Up Multipolar Surface Plasmon Polaritons by Collective Resonances in Arrays of Nanoantennas. *Phys. Rev. Lett.* **2010**, *105*, 266801.
(28) Kravets, V. G.; Schedin, F.; Taylor, S.; Viita, D.; Grigorenko, A. N. Plasmonic resonances in optomagentic metamaterials based on double dot arrays. *Opt. Express* **2010**, *18*, 9780−9790.
(29) Humphrey, A. D.; Barnes, W. L. Plasmonic surface lattice resonances in arrays of metallic nanoparticle dimers. *J. Opt.* **2016**, *18*, 035005.
(30) Omaghali, N. E. J.; Tkachenko, V.; Andreaone, A.; Abbate, G. Optical Sensing Using Dark Mode Excitation in an Asymmetric Dimer Metamaterial. *Sensors* **2014**, *14*, 272−282.
(31) Moritake, Y.; Kanamori, Y.; Hane, K. Experimental demonstration of sharp Fano resonances in optical metamaterials composed of asymmetric double bars. *Opt. Lett.* **2014**, *39*, 4057−4060.
(32) García de Abajo, F. J. *Colloquium*: Light scattering by particle and hole arrays. *Rev. Mod. Phys.* **2007**, *79*, 1267.
(33) Markel, V. A. Coupled-dipole approach to scattering of light from a one-dimensional periodic dipole structure. *J. Mod. Opt.* **1993**, *40*, 2281−2291.
(34) Zhou, S.; Janel, N.; Schatz, G. C. Silver nanoparticle array structures that produce remarkably narrow plasmon lineshapes. *J. Chem. Phys.* **2004**, *120*, 10871.
(35) Markel, V. A. Divergence of dipole sums and the nature of non-Lorentzian exponentially narrow resonances in one-dimensional periodic arrays of nanospheres. *J. Phys. B: At., Mol. Opt. Phys.* **2005**, *38*, L115.
(36) Humphrey, A. D.; Barnes, W. L. Plasmonic surface lattice resonances on arrays of different lattice symmetry. *Phys. Rev. B: Condens. Matter Mater. Phys.* **2014**, *90*, 075404.
(37) Moroz, A. Depolarization field of spheroidal particles. *J. Opt. Soc. Am. B* **2009**, *26*, 517−527.
(38) Lin, Q.-Y.; Li, Z.; Brown, K. A.; O'Brien, M. N.; Ross, M. B.; Zhou, Y.; Butun, S.; Chen, P.-C.; Schatz, G. C.; Dravid, V. P.; Aydin, K.; Mirkin, C. A. Strong Coupling between Plasmonic Gap Modes and Photonic Lattice Modes in DNA-Assembled Gold Nanocube Arrays. *Nano Lett.* **2015**, *15*, 4699−4704.
(39) *Handbook of Optical Constants*; Palik, E. D., Ed.; Academic Press: San Diego, CA, U.S.A., 1998.

DOI: 10.1021/acsphotonics.5b00727
ACS Photonics 2016, 3, 634−639